Article

Not peer-reviewed version

Theoretically Predicted and Experimentally Detected Chirality of Dibenzocycloctynes and of their Triazole Adducts with Azides.

Giulia Mazzoccanti , Roberta Franzini , Alessia Ciogli , Marco Pierini , Cristina Faggi , Antonio Francioso , Claudio Villani *

Posted Date: 19 January 2023

doi: 10.20944/preprints202301.0352.v1

Keywords: conformational chiralty; atropisomers; racemization; xray structure; circular dichroism; computational

Article

Theoretically Predicted and Experimentally Detected Chirality of Dibenzocycloctynes and of Their Triazole Adducts with Azides

Giulia Mazzoccanti [1] Roberta Franzini [1], Alessia Ciogli [1], Marco Pierini [1] and Cristina Faggi [2], Antonio Francioso [3] Claudio Villani [1,*]

[1] Department of Chemistry and Technology of Drugs, Excellence 2018-2022, Sapienza University of Rome, P.le Aldo Moro 5, 00185 Rome, Italy
[2] Department of Chemistry "Ugo Schiff", University of Florence, Via della Lastruccia 3–13, I-50019 Sesto Fiorentino, Italy
[3] Department of Biochemical Sciences, Sapienza University of Rome, P.le Aldo Moro 5, 00185 Rome, Italy

Abstract: Dibenzocycloctynes have emerged as a promising scaffold for bioorthogonal ligation. An important structural aspect that has not been addressed so far is connected with their chirality. Herein, we explore by theoretical and experimental methods this structural aspect that has been so far neglected. First, a computational analysis is conducted and results are used as a guideline for experimental investigation. Next, an array of different experiments (HPLC on chiral columns, chiroptical spectroscopy, X-ray diffraction) for structure elucidation are scrutinized in concert. Finally, this work demonstrates the chirality and the stereodynamic behavior of dibenzocycloctynes and of their triazole adducts with simple azides and uncover their conformational behavior.

Introduction

The chemistry of strained dibenzocyclooctynes derivatives continues to attract attention from a diverse array of scientists for several reasons [1–4]. The first is due to the considerable bond angle deformation of the triple bond to 163° corresponding to almost 18 kcal/mol of ring strain [5]. Addition of two phenyl rings to the structure increases further the angle strain. This destabilization of the ground state versus the transition state of the reaction causes a drastic rate acceleration compared to unstrained alkynes. The second is that the reaction proceeds at a rate that is sufficient for in vivo labeling while avoiding the use of the toxic copper(I) catalysts traditionally employed in "click chemistry" with terminal alkynes ("copper-free click Chemistry") [6]. The third feature of dibenzocyclooctynes chemistry is related to its bioorthogonality thus allowing to probe biomolecules in living organisms without interacting or interfering with biological systems [7–9].

All of these aspects of the dibenzocycloalkyne reaction with azides result in a multi opportunity synthetic approach that is revolutionizing the chemistry and biochemistry of ligation, allowing for several synthetic approaches that are rich and varied. Thus, the field of bioorthogonal chemistry of strained cyclooctynes is definitely recognized as an inspiring cutting edge of reaction methodology and an important new chemical tool for biological discovery [10].

Yet, the conformational chirality of these fascinating molecules and of their triazole adducts with azides have not been studied so far.

Results and Discussion

Here we report a detailed structural and dynamic study of **1-5** DiBenzoCyclooctynes (**DBC**, Scheme 1) and of their triazole adducts with simple azides (Scheme 2).

Preprints (www.preprints.org) | NOT PEER-REVIEWED | Posted: 19 January 2023 doi:10.20944/preprints202301.0352.v1

Scheme 1

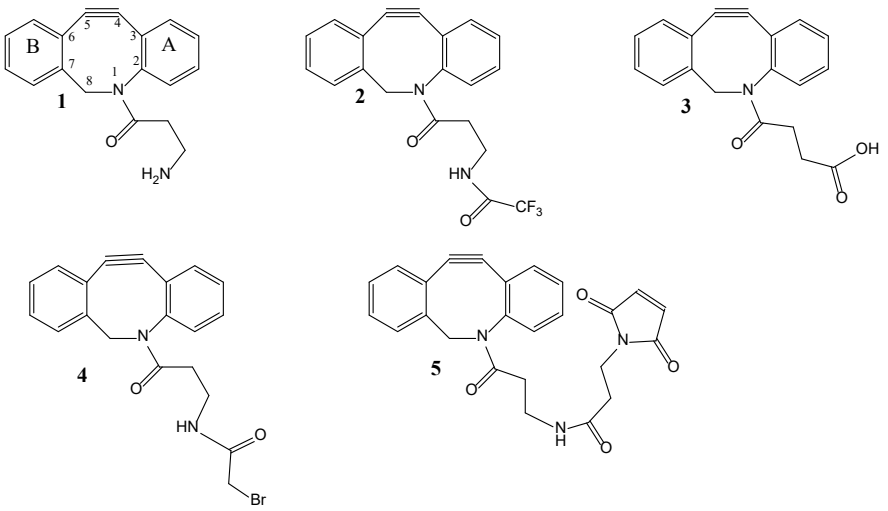

Scheme 1. Structures of investigated **1-5** dibenzocyclooctynes.

For the exploratory survey of key experimental structural features of cyclooctynes we employed compound **2** as the test substrate.

Conformational analysis of **2**, performed at the molecular mechanic level of theory with the MMFF94 force field [11], showed that this one is a conformationally rigid molecule in its tricyclic framework including the amide group (hereafter denoted with the acronim **DBC-Amd**), with the carbonyl oxygen of this latter one projected above the phenyl ring A and pointing towards one of the hydrogens on C8 in 99.7% of the populated conformations, inside an energetic gap of 3.6 kcal/mol. In particular, the cyclooctyne core adopts a chair conformation, with the alkyne C4, C5 carbon atoms and the ring nitrogen atom almost coplanar with phenyl ring A, whereas C8 and ring B lye below the A ring plane (Figure 1).

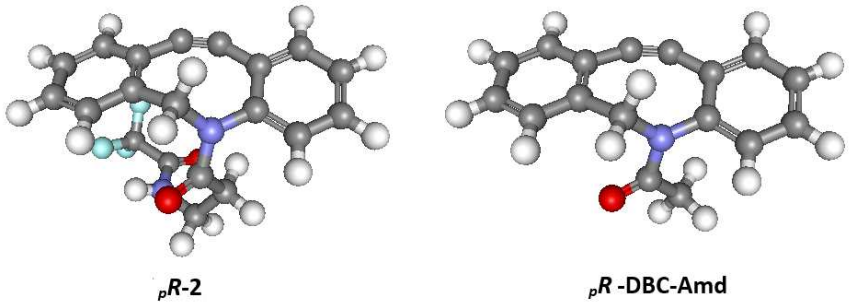

Figure 1. Low energy structures of $_pR$**-2** and $_pR$ **-DBC-Amd** obtained by calculation, at the molecular mechanic and DFT level of theory, respectively.

The angle between the planes containing the two phenyl rings A and B is about 16°. Due to non-planarity of the **DBC-Amd** framework and to its asymmetric substitution pattern, **1-5** are devoid of any reflection type symmetry element and are thus chiral. It is anticipated that enantiomer interconversion can occur in these molecules by a ring flip process. Thus, in order to theoretically analyze the stereodynamic pathways for enantiomer interconversion (enantiomerization) of the synthesized **1-5** dibenzocyclooctynes, on the simplified structure common to all these ones (i.e. on the **DBC-Amd** scaffold), we performed DFT optimization of both ground and transition states related to its ring flipping pathway, carried out at the B3LYP/6-31G(d) [12] level of theory. Indeed, it is reasonable to expect that the amide arms linked to the **DBC-Amd** framework in derivatives **1-5**

Preprints (www.preprints.org) | NOT PEER-REVIEWED | Posted: 19 January 2023 doi:10.20944/preprints202301.0352.v1

cannot significantly influence their stereochemical lability. The estimated enantiomerization energy barrier, $\Delta E_{en}^{\#}$, is of 24.1 kcal/mol, to which correspond a half-life time around 58 h at room temperature. Based on this information, which indicates a rather large enantiomerization barrier, we were able to plan the experimental conditions to physically separate the enantiomers of **1-5**. Accordingly, the enantiomers of **1-5** were easily resolved by HPLC using the Pirkle-type (*R*,*R*)-Whelk-O1[13] chiral stationary phase. Elution with hexane/CH2Cl2/MeOH 80:20:2 gave two nicely resolved peaks corresponding to the ($_P$***R***)- and ($_P$***S***)-enantiomers of **2**, with elution times of 8.0 and 11.5 min, respectively. When monitored by CD detection at 290 nm, bisignate peaks of equal area were observed, as expected for a racemate.

The large enantioselectivity values (α = 1.80-x.xx, Supporting Information, pages 2–4) obtained at analytical level on a 250 · 4.6 mm column, and the good solubility of **1-5** in the eluent allowed for a simple scale up at preparative levels on the 250 × 10 column. Enantioselectivity and peak shapes remained unchanged even at high column loading (15 mg per run) thus enabling very efficient fraction collection in terms of speed of separation, enantiomeric purity and overall yield. As a result, about 20 mg of each enantiomer of **1-5** were obtained after iterative HPLC separations and solvent removal from the pooled fractions. The individual enantiomers collected by chiral HPLC showed enantiomeric excesses greater than 99.5%, as determined by analytical HPLC.

With discrete amounts of the single enantiomers of **1-5**, we performed thermal racemization experiments to evaluate their stereochemical stabilities.

Thermal racemization of the enantiomers of **1-5** in the HPLC eluent at 50 °C was monitored by HPLC following the decay of the enantiomeric excess over time, and racemization rate constants value between k_{rac} = 0.0033 min^{-1} and k_{rac} = 0.0087 min^{-1} (T = 50 °C) were determined (Supporting Information). A statistical transmission coefficient γ = 0.5 was used in the calculation of the free energy barrier $\Delta G^{\ddagger}$ from the rate constant of the process. This gave values of racemization activation energies between 24.82 ± 0.1 kcal/mol and 24.20 ± 0.1 kcal/mol at 50 °C and are consistent with the computational study.

These barriers translate into half-lives between 1.5 and 4 days at 25 °C, thus indicating that **1-5** are atropisomeric at room temperature.

The pure enantiomers of **1-5** were characterized by polarimetry and electronic circular dichroism spectroscopy. The first eluted enantiomers of **1-5** give positive rotation at the sodium D line in chloroform solution, e.g (+)-**2**: $[\alpha]^{30}_D$ = +319. Its circular dichroism spectrum (methanol solution) exhibits positive bands at 233 nm and 270-320 nm, the last showing vibronic signature. The second eluted enantiomer gives a mirror image CD spectrum (Figure 2) and negative rotation at the sodium D line in chloroform solution, (-)-**2**: $[\alpha]^{30}_D$ = −319.

The electronic circular dichroism (ECD) spectra of **1-5** are very similar, showing the same pattern of positive bands for the first eluted enantiomers having positive optical rotations at the sodium D line (see Supporting Information).

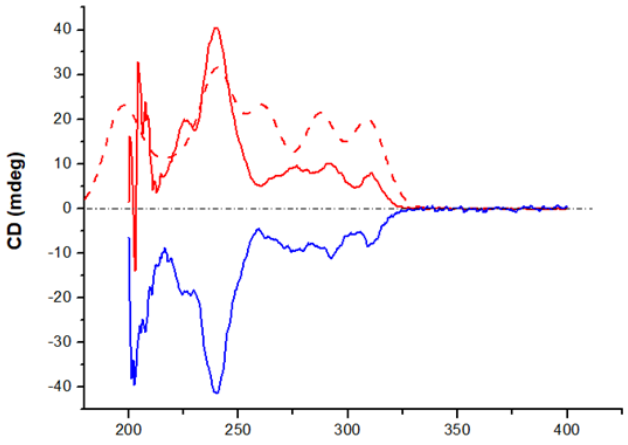

Figure 2. Experimental ECD spectra of (+)-**2** (red) and (-)**2** (blue). The calculated ECD spectrum of $_P$***R*-DBC-Amd** is superimposed as red dashed line.

Preprints (www.preprints.org) | NOT PEER-REVIEWED | Posted: 19 January 2023 doi:10.20944/preprints202301.0352.v1

Starting from these results, the absolute configuration (AC) of **2** was determined by comparing the experimental ECD spectra of its two chromatographically resolved enantiomers with the one assessed for the $_p$***R*** optical isomer of the above quoted **DBC-Amd** framework, a methodology used previously in determining the ACs of chiral-chromatography-resolved enantiopure molecules[14]. This was carried out by submitting the $_p$***R*-DBC-Amd** structure to new optimization and, next, to frequencies calculation at a suitable density functional level of theory (DFT), which led to the computed ECD spectrum shown in Figure 2.

The predicted ECD spectrum of $_p$***R*-DBC-Amd** is in excellent qualitative agreement with the experimental ECD spectrum of **(+)-2**, leading to the conclusion that the absolute configuration of this enantiomer (and therefore, also of the (+)-enantiomers of the other **DBC** derivatives) is unambiguously **(+)-**$_p$***R***. Further support for the reliability of the DFT calculations for **2** is provided by the X-ray structure of **4**. Crystals of the second eluted enantiomer (-)**4**, $[\alpha]^{25}_D = -319$, suitable for X-ray analysis, were grown from a hexane/CH_2Cl_2 solution. The 2-bromoacetyl group was chosen to facilitate the AC assignment by the X-ray diffraction analysis. The molecular structure revealed by the X-ray diffraction study is reported in Figure 3. The general geometrical features of (-)-**4** are very similar to those obtained by calculation for **2**. The second eluted, (-)-**4**, exhibits a slightly distorted chair conformation of the eight-membered ring, with the nitrogen and C4 and C5 atoms almost coplanar with the phenyl ring and the carbonyl oxygen projected away from the phenyl ring and pointing towards one of the H atoms of the C8 methylene unit (amide adopting the *E* configuration). The absolute configuration is unambiguously determined as **(-)-**$_p$***S***, in agreement with the AC determined by comparison of experimental and calculated ECD spectra (Figure X).

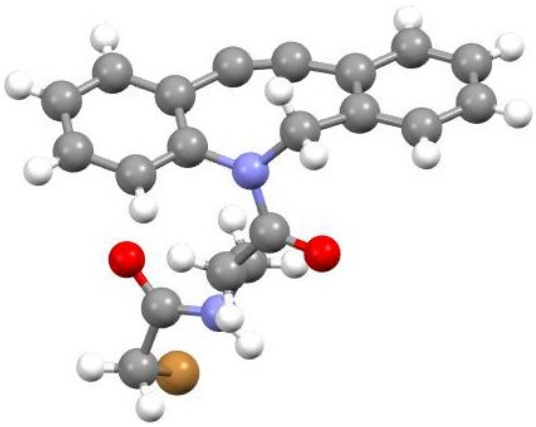

Figure 3. Structure of $_p$***S***-(-)-**4** obtained by X-ray diffraction analysis.

Having addressed the general structural properties of cyclooctynes **1-5** and having established their atropisomeric nature at room temperature, we were in a position to investigate the structural properties of the corresponding triazole obtained by reaction with simple azides.

Reaction of cyclooctynes **2** with either phenyl (**Ph**) or benzyl (**Bz**) azides proceeds smoothly to yield the two regioisomeric triazoles **2Ta** (**2TaPh** with R=**Ph** and **2TaBz** with R=**Bz**) and **2Tb** (**2TbPh** with R=**Ph** and **2TbBz** with R=**Bz**) (**Scheme 2**).

Preprints (www.preprints.org) | NOT PEER-REVIEWED | Posted: 19 January 2023 doi:10.20944/preprints202301.0352.v1

Scheme 2

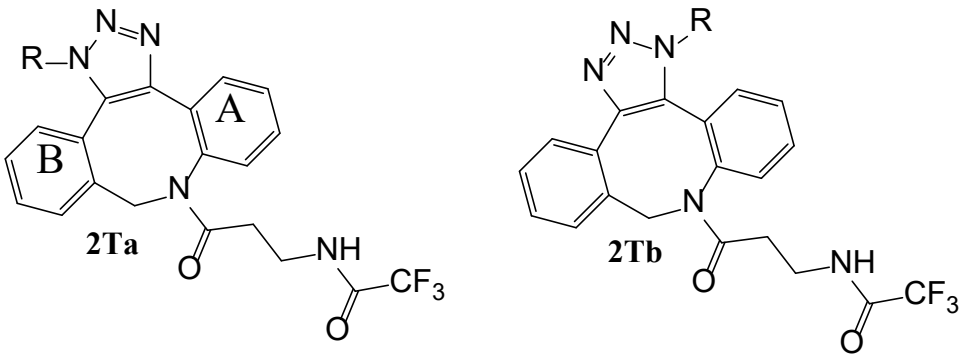

Scheme 2. Structures of regioisomeric triazoles derived from cyclooctyne **2**. R = **Ph** or **Bz**.

Conformational analysis, carried out in three steps, first by molecular mechanics search method, next by further optimization of all the obtained conformations at a low Hartree-Fock level of theory and, finally, by single point energy evaluation of all the geometries at the Density Functional B3LYP/6-31G(d) level of Theory (DFT), showed **2TbBz** to be a conformationally flexible molecule that enjoys a greater conformational freedom compared to its precursor **2**. Compound **2TbBz** adopts a structure that is chiral as well for the presence of an asymmetry plane related to its tetracyclic framework that also includes the amide group and the **Bz** substituent (a structural fragment hereafter denoted with the acronim **DBCT-Amd-bBz**). Cycloaddition reaction released the angle strain of the starting cyclooctynes, resulting in a minimum energy conformation with a bent structure, the angle between the phenyl planes now amounting to about 80°. Inspection of the energy landscape of **2TbBz** showed the presence of four different conformations available to the **DBCT-Amd-bBz** framework: the two more stable ones have very similar energetic stability (within 0.34 kcal/mol) but different spatial disposition of **Bz** with respect to the triazole plane (in front of, **2TbBz-F**, or behind of such plane, **2TbBz-B**), with the amide group always showing *E* disposition (**2TbBz-F-*E*** and **2TbBz-B-*E***); the other two have the structure similar to the previous couple about the **Bz** spatial disposition, but show the amide group flipped in *Z* configuration (**2TbBz-F-*Z*** and **2TbBz-B-*Z***, respectively). This configurational-change of the amide portion increases by 1.6 kcal/mol the instability computed passing from the **2TbBz-F-*E*** to the **2TbBz-F-*Z*** structure and of 3.8 kcal/mol from **2TbBz-B-*E*** to **2TbBz-B-*Z*** (the Boltzmann populations for the global *E* and *Z* configurations of **2TbBz** are 96% and 4%, respectively).

Chromatography on silica allowed to resolve the two regioisomeric triazoles **2TaBz** and **2TbBz**. Crystals suitable for **X-ray** analysis were grown for the first eluted regioisomer **2TbBz** from a hexane/CH_2Cl_2 solution. Such **X-ray**-diffraction determination revealed the presence in the analyzed crystal of the structure reported in Figure 4 (right side), which is very similar to the species **2TbBz-F-*E***, that is to say, to one of the two more stable conformers obtained by computation, the one displaying the benzyl ring in front of the triazole plane and the amide group in *E* configuration (Figure 4, left side).

Preprints (www.preprints.org) | NOT PEER-REVIEWED | Posted: 19 January 2023 doi:10.20944/preprints202301.0352.v1

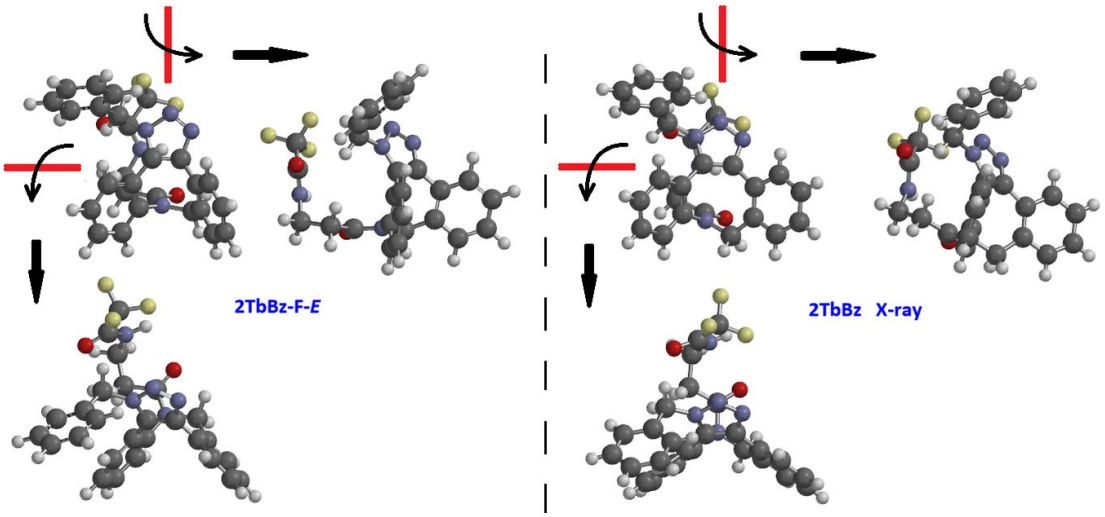

Figure 4. Left, low energy structure of **2TbBz-F-*E*** obtained by calculation, right X-ray diffraction structure of **2TbBz**.

Theoretical assessment and experimental determination of the activation barriers governing the enantiomerization of compounds 2TaPh, 2TaBz, 2TbPh and 2TbBz: enantiomers of 2TaPh, 2TaBz, 2TbPh and 2TbBz are not atropisomeric at room temperature.

Theoretical Assessment of $\Delta E_{en}^{\#}$ Activation Barriers

On the base of the good result obtained by theoretical approach about the estimation of the enantiomerization barrier that opposes the interconversion of the optical isomers of **DBC 2** (a difference lesser than 1 kcal/mol from the experimental data), equivalent DFT calculations have been extended in the evaluation of the same type of process concerning the species **2TaPh**, **2TaBz**, **2TbPh** and **2TbBz**. The adopted procedure was based on the following steps: (1) conformational search performed at the molecular mechanics level of theory of the four frameworks **2DBCT-Amd-aPh**, **2DBCT-Amd-aBz**, **2DBCT-Amd-bPh** and **2DBCT-Amd-bBz**, followed by further optimization of all the obtained structures at a semiempirical level of theory; (2) prediction of the **DBCT** ring flipping pathway profile performed at semiempirical level of theory starting from the Global Minimum, GM, found by the search carried out in step 1; (3) DFT optimization, performed at the B3LYP/6-31G(d) level of theory, of both ground and transition states related to the ring flipping pathway analyzed in step 2.

The obtained results can be summarized as follows: (a) **2DBCT-Amd-aPh**, $\Delta E_{en}^{\#}$ = 16.56 kcal/mol; (b) **2DBCT-Amd-aBz**, $\Delta E_{en}^{\#}$ = 16.97 kcal/mol; (c) **2DBCT-Amd-bPh**, $\Delta E_{en}^{\#}$ = 13.70 kcal/mol; (d) **2DBCT-Amd-bBz**, $\Delta E_{en}^{\#}$ = 15.15 kcal/mol. At temperature of 25 °C these $\Delta E_{en}^{\#}$ data correspond to enantiomerization half-life times $\mathbf{t}_{1/2}^{en}$ of 0.15 s, 0.31 s, 0.001 s and 0.014 s, respectively.

Experimental Determination of $\Delta G_{en}^{\#}$ Activation Barriers

Coherently with the theoretical assessments quoted in the above subparagraph, the attempted HPLC resolution of the enantiomers of **2TaPh**, **2TaBz**, **2TbPh** and **2TbBz** at room temperature on the Welk-O1 chiral stationary phase failed due to fast on column enantiomerization. However, after reduction of the column temperature up to −50 °C, deconvolution and split peaks for the enantiomers of **2TaPh**, **2TaBz** and **2TbBz**, but not for **2TbPh**, were observed, with the generation of dynamic chromatograms in which, between the resolved peaks, classical plateau zones are clearly visible (see Supporting Information). This behavior is consistent with the $\mathbf{t}_{1/2}^{en}$ values estimated for the frameworks **2DBCT-Amd-aPh**, **2DBCT-Amd-aBz**, **2DBCT-Amd-bPh** and **2DBCT-Amd-bBz** at the temperature of −50 °C: 41 min; 104 min; 0.06 min; 2 min, respectively. Thus, simulation of the exchange deformed peaks via stochastic model yielded the apparent rate constants, and so, also the

Preprints (www.preprints.org) | NOT PEER-REVIEWED | Posted: 19 January 2023 doi:10.20944/preprints202301.0352.v1

related free energy barriers for the on-column enatiomerization [15–20], which at −40 °C correspond (in kcal/mol) to 16.08 for **2TaPh**, 16.66 for **2TaBz** and 15.99 for **2TbBz** (see Supporting Informationrmation for results obtained at other temperatures). Taking into consideration that for the monomolecular flipping process of the **DBCT** tetracyclic frameworks it is not expected a significant entropy variation, it is also expected that the experimental $\Delta G_{en}^{\#}$ values are scarcely affected by changes of temperature, and that therefore, within a restricted range of temperature, these data may directly approach the relevant enthalpy changes, $\Delta H_{en}^{\#}$. This should make the existing relationship among experimental $\Delta G_{en}^{\#}$ and computed $\Delta E_{en}^{\#}$ quantities relatively independent of temperature.

Interestingly, the experimental values of $\Delta G_{en}^{\#}$ determined for **2TaBz** at the temperatures of −30 °C (16.78 kcal/mol), −35 °C (16.87 kcal/mol) and −40 °C (16.66 kcal/mol) resulted substantially not influenced by these changes, thus giving direct evidence of a negligible entropy effect. On the base of all these evidences and considerations, $\Delta G_{en}^{\#}$ values achieved at all the explored temperatures for compounds **2, 2TaPh**, **2TaBz** and **2TbBz** have been plotted against the relevant computed $\Delta E_{en}^{\#}$ values (Figure 5).

T °C		$\Delta G^{\#}$	$\Delta E^{\#}$	err. %
50	1	24.82	24.13	1.4
50	2	24.61	24.13	0.5
50	3	24.20	24.13	-1.2
50	4	24.54	24.13	0.2
50	5	24.50	24.13	0.1
-40	2TaBz	16.66	16.97	-3.9
-35	2TaBz	16.87	16.97	-2.6
-30	2TaBz	16.78	16.97	-3.1
-40	2TaPh	17.08	16.56	1.1
-30	2TaPh	17.13	16.56	1.4
-40	2TbBz	15.99	15.15	3.2
-50	2TbBz	15.87	15.15	2.5
	2TbPh		13.70	
-30	2TbPh-AMD1	17.95	17.13	2.7
-25	2TbPh-AMD1	18.03	17.13	3.1

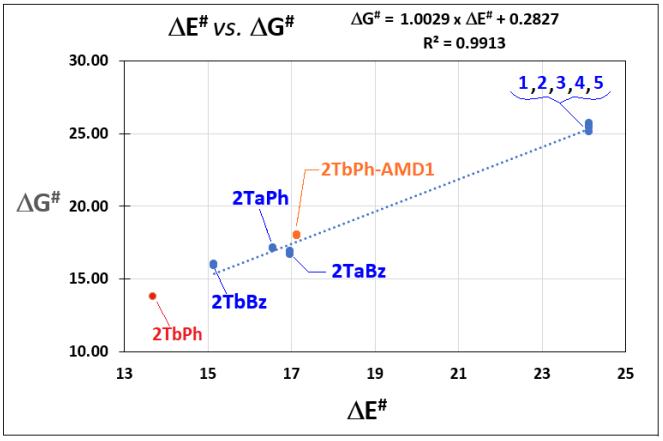

Figure 5. Linear correlation existing between experimental and calculated activation barriers relevant to the enantiomerizzation of compounds **2, 2TaPh**, **2TaBz** and **2TbBz** and **AMD1**-diastereomerizzation of compound **2TbPh**.

Inspection of this plot clearly highlights the very good linear correlation existing among the $\Delta G_{en}^{\#}$ and $\Delta E_{en}^{\#}$ data, characterized by $R^2 = 0.9913$, a result that strongly supports the reasons in favor of enthalpy-driven enantiomerization processes. In addition, the same good fit also affords a clear indication about the excellent reliability afforded by the chosen DFT calculations in predicting the activation barriers of enantiomerization involved within the here studied typology of molecules.

The dynamic HPLC plot of **(4?)2TbPh** is more complex than expected. On the Welk-O1 column **(4?)2TbPh** shows only a single averaged peak at near room temperature, which splits in two peaks of strongly different areas at lower temperature (i.e., interconversion between non-enantiomeric species, according to the very low $\Delta E_{en}^{\#}$ of 13.70 kcal/mol estimated for this species by calculation), in slow exchange regime, with a visible plateau that connect the two species in the temperature range -10 ÷ -20°C. The existence of two interconverting species is also confirmed by HPLC on silica, where two peaks of unequal intensities (2.9 ratio at T=-60°C) were observed at low temperature, that eventually coalesce in a single peak at higher temperatures. Simulation of HPLC plots obtained either on the chiral or achiral column gave the rate constants of interconversion $k_{dr1\text{-}2}/k_{dr2\text{-}1}$ and the related $\Delta G^{\#}_{dr1\text{-}2}/\Delta G^{\#}_{dr2\text{-}1}$ values for the first and second eluted diastereomers (chiral column: T= −40 °C; $k_{1\text{-}2} = 0.32$ min^{-1}, $\Delta G^{\#}$ = 15.95 ± 0.1kcal/mol, $k_{2\text{-}1} = 0.266$ min^{-1}, $\Delta G^{\#}$ = 15.99 ± 0.1kcal/mol, achiral column: T= −25 °C; $k_{dr1\text{-}2} = 0.040$ min^{-1}, $\Delta G^{\#}_{dr1\text{-}2}$ = 18.03 ± 0.1 kcal/mol; $k_{dr2\text{-}1} = 0.100$ min^{-1}, $\Delta G^{\#}_{dr2\text{-}1}$ = 17.62 ± 0.1 kcal/mol; T= −30 °C; $k_{dr1\text{-}2} = 0.022$ min^{-1}, $\Delta G^{\#}_{dr1\text{-}2}$ = 17.95 ± 0.1 kcal/mol; $k_{dr2\text{-}1} = 0.057$ min^{-1}, $\Delta G^{\#}_{dr2\text{-}1}$ = 17.50 ± 0.1 kcal/mol) (see Supporting Informationrmation). Such diastereomeric interconversion could be attributed, in

principle, to the change from the ***E*** to the ***Z*** configuration of one of the two amide groups within the arm linked to the **2DBCT-Amd** framework of **(4?)2TaPh**, that which is part of the tetracyclic structure (**AMD1**), the other located at the terminal of chain (**AMD2**). Information on this has been obtained by theoretical approach. Activation barrier of diastereomerization for the change from the ***E*** to the ***Z*** configuration of both the **AMD1** and **AMD2** amide groups ($\Delta E^{\#}_{dr1\text{-}2}$ values), within the **2TbPh** structure, has been assessed by DFT optimization (again performed at the B3LYP/6-31G(d) level of theory) of the both ground and transition states relevant to the processes. The obtained results indicated that isomerization of **AMD1** has an activation barrier 4.2 kcal/mol smaller than that of **AMD2** (i.e., 17.13 against 21.31 kcal/mol, respectively), presumably thanks to the conjugation that this can be established with the tetracyclic structure of which it is part. Through comparison of these ones with the experimental $\Delta G^{\#}_{dr1\text{-}2}$ values determined at −25 and −30 °C (Figure 5), it seems completely reasonable to affirm that the observed diastereomerization of **2TbPh** is attributable to the ***E*** to ***Z*** flip of the **AMD1** amide group, conclusion that is also supported by the good fit that the values of $\Delta G^{\#}_{dr1\text{-}2}$ and $\Delta E^{\#}_{dr1\text{-}2}$ show in the above already discussed linear correlation reported in Figure 5.

Conclusion

The chirality of dibenzocycloctynes **1-5** has been first predicted by computational methods and then confirmed by chiral HPLC, chiroptical spectroscopy and X-ray diffraction analysis. **1-5** are atropisomeric at room temperature, and enantiomer interconversion occurs via a ring flip process. Parallel computational investigations carried out on the triazole adducts with phenyl or benzyl azides, show the triazoles to be chiral as well, albeit with a lower activation energy for the enantiomerization process. Chiral and achiral HPLC at variable column temperature demonstrated the dynamic behavior of the flexible triazoles and disclosed the activation parameters for their enantiomerization during cryo-chromatography.

Author Contributions: R.F., G.M, A.F. and A.C. performed the experiments, edited the manuscript and treated the data. M.P performed computational calculations and wrote the relevant part of the manuscript. C.F performed X-ray analysis. C.V. proposed the research project, provided resources, designed the experiments, wrote and edited the manuscript.

Ethics Declarations: Competing interests. The authors declare no competing interests.

References

1. Ess, D., Jones, G. O. H., Houk, K. N. Transition States of Strain-Promoted Metal-Free Click Chemistry: 1,3-Dipolar Cycloadditions of Phenyl Azide and Cyclooctynes. *Org. Lett*. 2008, **10**, 8, 1633–1636
2. Schoenebeck,F., Ess, D.H, Jones, G.O., Houk, K.N. Reactivity and Regioselectivity in 1,3-Dipolar Cycloadditions of Azides to Strained Alkynes and Alkenes: A Computational Study. *J. Am. Chem. Soc*. 2009, **131**, 23, 8121–8133
3. Bach, R.D., Ring Strain Energy in the Cyclooctyl System. The Effect of Strain Energy on [3 + 2] Cycloaddition Reactions with Azides. *J. Am. Chem. Soc*. 2009, **131**, 14, 5233–5243
4. Yavari, I., Nasiri, F.A., Djahaniani _H., Jabbari A., Ab Initio Molecular Orbital Study of Conformational Properties of Cyclohexyne, Cycloheptyne, and Cyclooctyne. *Int. J. Quantum Chem*., **106**, 697–703 (2006)
5. Meier, H., Petersen, H. Kolshorn, H, Die Ringspannung von Cycloalkinen und ihre spektroskoyischen Auswirkungen. *Chem. Ber*. **113**, 2398 - 2409 (1980)
6. Steflova, J. Storch G., Wiesner, S. Stockinger, S. Berg, R., Trapp O., Investigation of Strain-Promoted Azide–Alkyne Cycloadditions in Aqueous Solutions by Capillary Electrophoresis. J. Org. Chem. **83**, 2018, 604–613.
7. Sletten, E. M., Bertozzi, C. R., From Mechanism to Mouse: A Tale of Two Bioorthogonal Reactions, *Acc. Chem. Res*., **44**, 9, 666–676, (2011).
8. Agard, N. J., Prescher, J. A., Bertozzi C. R., A Strain-Promoted [3 + 2] Azide–Alkyne Cycloaddition for Covalent Modification of Biomolecules in Living Systems. *J. Am. Chem. Soc*., **126**, 46, 15046–15047,(2004)
9. Debets, M. F., van Berkel, S. S., Dommerholt, J., Dirks, A. J., Rutjes, F. P. J. T, van Delft F. L., Bioconjugation with Strained Alkenes and Alkynes. *Acc. Chem. Res*., **44**, 9, 805–815,(2011)
10. Devaraj, N. K., The Future of Bioorthogonal Chemistry. *ACS Cent. Sci*., 4, 8, 952–959, (2018)
11. MMFF94 force field
12. B3LYP/6-31G(d)

13. 13 Pirkle, W.H.; Welch, C.J.; Lamm, B. Design, Synthesis, and Evaluation of an Improved Enantioselective Naproxen Selector. *J. Org. Chem*., **57**, 3854–3860, (1992).
14. Stephens, P. J., Devlin, F. J., Gasparrini, F., Ciogli, A., Spinelli, D., Cosimelli B., Determination of the Absolute Configuration of a Chiral Oxadiazol-3-one Calcium Channel Blocker, Resolved Using Chiral Chromatography, via Concerted Density Functional Theory Calculations of Its Vibrational Circular Dichroism, Electronic Circular Dichroism, and Optical Rotation. *J. Org. Chem*., **72**, 13, 4707–4715, (2007)
15. Gasparrini,F, Misiti,D., Pierini, M., Villani, C., Enantiomerization barriers by dynamic HPLC. Stationary phase effects, *Tetrahedron: Asymm*., **8**, Issue 12, 2069-2073, (1997)
16. Trapp, O. Unified Equation for Access to Rate Constants of First-Order Reactions in Dynamic and On-Column Reaction Chromatography. *Anal. Chem*. 2006, 78, 189–198.
17. Villani, C.; Pirkle, W.H. Chromatographic resolution of the interconverting stereoisomers of hindered sulfinyl and sulfonyl naphthalene derivatives. *Tetrahedron Asymm.* 1995, 6, 27–30.
18. Mortera, S.L.; Sabia, R.; Pierini, M.; Gasparrini, F.; Villani, C. The dynamic chromatographic behavior of tri-o-thymotide on HPLC chiral stationary phases. *Chem. Commun.* **2012**, *48*, 3167–3169.
19. Franzini, R.; Rosetti, A.; Villani, C. Low Temperature Dynamic Chromatography for the Separation of the Interconverting Conformational Enantiomers of the Benzodiazepines Clonazolam, Flubromazolam, Diclazepam and Flurazepam. *Symmetry* **2021**, *13*, 1012
20. Sabia, R., Ciogli, A. Pierini, M., Franzini, R., Iazzetti, A., Villani, C.
21. Chromatographic separation of the interconverting enantiomers of imidazo- and triazole-fused benzodiazepines, *J. of Chromatogr. A*, Vol 1647, 2021, 462148